International Journal of Pharma Professional's Research (IJPPR)
(A Peer Reviewed Journal of Pharmacy)
ISSN (Online): 0976-6723 ISSN (Print): 2249-3948

Development of Cefuroxime axetil-loaded lipid nanoparticles for superior antimicrobial and antibiofilm Efficacy

Reetika Rawat[1]*, Shipra Sharma[1,2], Parul Gupta[1], Ayush Rawat[1], Medhavi Gupta[1], Prashant Upadhyay[3]

[1]Shri Ram Murti Smarak, College of Engineering and Technology, Bareilly, 243202, India.
[2]Faculty of Pharmacy, IFTM University, Moradabad, 244102, India.
[3]School of Pharmaceutical Sciences, Faculty of Pharmacy, IFTM University, Moradabad-244102, Uttar Pradesh, India

Doi: 10.69580/IJPPR.17.1.2026.99-122

ABSTRACT

Introduction: The current research aims to formulate lipid nanoparticles (LNs) to enhance the bioavailability and antimicrobial efficacy of Cefuroxime axetil (CA).

Material and methods: Cefuroxime axetil-loaded lipid nanoparticles were fabricated utilizing the hot homogenization process and characterized for particle size (335.11 ± 25.40 nm), zeta potential (-30.64 ± 3.58), encapsulation efficiency (86.02 ± 2.73), surface morphology, and in vitro drug release.

Results: Characterization was performed via differential scanning calorimetry, and infrared spectroscopy confirmed successful encapsulation of CA within the lipid matrix. Optimized formulation showed smooth and spherical morphology, with sustained drug release for 24 h.

Discussion: in-vitro antibiofilm activity showed higher efficacy of CA-LNs, achieving biofilm eradication at lower concentrations (35 µg/ml against E. coli) compared to free CA (130 µg/ml against E. coli), as verified by SEM imaging.

Conclusion: Conclusively, CA-LNs provide a promising delivery system for enhancement of oral bioavailability and therapeutic efficacy of CA in the treatment of intracellular infections.

Keywords: Nanostructures, biofilm, encapsulation efficiency, drug delivery, anti-microbial, lipid carriers.

Corresponding Author- Reetika Rawat, Shri Ram Murti Smarak, College of Engineering and Technology, Bareilly, 243202, India
reetikarawat32@gmail.com
Volume 17, Issue 1, 2026, Received: 15 Nov. 2025, Accepted: 5 Jan 2026, Published: 31 Jan 2026

1. Introduction

Biofilm-forming pathogens, such as *Staphylococcus aureus*, *Haemophilusinfluenzae*, *Streptococcus pneumoniae*, and *Enterobacteriaceae,* are extensively involved in nosocomial infections. These biofilms contain bacteria that remain embedded in an exopolysaccharide matrix, resulting in 1000-fold greater antibiotic resistance in comparison to their planktonic state. [1-4] This antibiotic resistance enhances the burden on healthcare systems, thus affecting the quality of life of patients. According to the current scenario, bacterial co-infections associated with severe SARS-CoV-2 pneumonia, particularly in ICU patients, has further enhanced this challenge, affecting airways and lung structures. [5-8] Thus, there is an urgent requirement for innovative microbial therapies to treat biofilm-associated infections. Literature survey revealed cephalosporin antibiotics efficacy for *in-vitro* and *in-vivo* antibiofilm activity, as alone as well as for combination therapies. [9,10]

Cefuroxime axetil, a cephalosporoin antibiotic is effectively used as drug of choice for lower respiratory tract infections due to its stability in acidic milieu of stomach.[11] Limitations associated with cefuroxime axetil such as lower aqueous solubility, systemic bioavailability, extensive first pass metabolism and higher dose frequency due to lower half-life (3-5 h) limits its therapeutic efficacy in biofilm intracellular infections. [12] Some conventional formulations are available such as, tablets and suspensions, that shows limited efficacy for enhancement of palatability, bioavailability, therapeutic efficacy and reducing hepatotoxicity of drug. [13]

Various advances in nanotechnology field facilitate promising solutions for enhanced efficacious oral drug delivery systems. Among them, lipid nanoparticles (LNs), composed of lipids like waxes, fatty acids, and glycerides that solidifies at room temperature, offers many benefits, including enhanced bioavailability, stability, drug payload and their commercial scalability. [14, 15]

The size and excipient composition of nanostructured lipid carriers enables lymphatic uptake through paracellular and transcellular pathways, bypassing portal circulation and reducing first-pass metabolism. [16-18] Moreover, lipophilicity of nanostructured lipid carriers enables direct interaction with complex structure of biofilm inhibiting various stages of biofilm formation. [19-21] LNs in lyophilized form can be encapsulated into capsules, pellets or tablets for practical utilization.

The current study is focused to develop cefuroxime axetil-loaded lipid nanoparticles (CA-LNs) utilizing the hot homogenization method. Formulation optimization was performed on the basis of formulation variables andprocess variables including particle size, zeta potential, polydispersity index (PDI) and encapsulation efficiency to achieve optimized formulation. The optimized formulation was further characterized for morphology, *in-vitro* drug release, and solid- phase properties. Moreover, the *in-vitro* antimicrobial activity against *Escherichia coli*was evaluated to assess the therapeutic potential of the formulation.

2. Materials and methods

Corresponding Author- Reetika Rawat, Shri Ram Murti Smarak, College of Engineering and Technology, Bareilly, 243202, India
reetikarawat32@gmail.com
Volume 17, Issue 1, 2026, Received: 15 Nov. 2025, Accepted: 5 Jan 2026, Published: 31 Jan 2026

2.1 Materials

Cefuroxime axetil was supplied as a gift sample by Ranbaxy Laboratories Ltd., New Delhi, India. Pluronic F-68 (PF-68), soya lecithin, stearic acid, Compritol 888 ATO, and dialysis membranes were procured from HiMedia (Mumbai, India). HPLC-grade water, acetonitrile, and Tween 80 were obtained from Merck, Germany. IL-6 and TNF-α kits were sourced from BD Biosciences (Minneapolis, MN). All the received materials were used as such without any further purification and distilled water was utilized throughout the study.

2.1.1 Development of cefuroxime axetil-loaded lipid nanoparticles (CA-LNs)

Cefuroxime axetil-loaded lipid nanoparticles were fabricated, using modified hot homogenization method. For the process, Compritol 888 ATO, stearic acid and soya lecithin were melted at 5-10 °C above their melting points and mixed to form the lipid phase. Drug was dissolved in the melted lipid to formate the oil phase. Alongside, an aqueous phase was prepared by dissolvingPluronic F-68 (0.5% w/v) in water and heating to 70 ± 2 °C.Further, oil phase was then added further to the aqueous phase and emulsified by homogenization process at 125,000 rpm for 20 minutes. Emulsion was cooled after that along with stirring.Carrying forward the process, dispersion was centrifuged at 25,000 rpm at 4°C for 20 minutes to attain the collected nanoparticle pellet, which was then redispersed in distilled water consisting 10% w/vmannitol as a cryoprotectant. The resultant dispersion was frozen at -60 °C overnight and lyophilized at -55 °C under 0.07 bar pressure for 48 hours to achieve fine, dry CA-LNs. Various batches were prepared to optimize formulation and process variables, as detailed in Table 1.

Table 1: Optimization table with process and excipients variables.

Corresponding Author- Reetika Rawat, Shri Ram Murti Smarak, College of Engineering and Technology, Bareilly, 243202, India
reetikarawat32@gmail.com
Volume 17, Issue 1, 2026, Received: 15 Nov. 2025, Accepted: 5 Jan 2026, Published: 31 Jan 2026

F.code	Soya lecithin (mg)	Comp ritol (mg)	Stearic acid (mg)	Pluronic F-68 (%w/v)	Pluronic F-127 (%w/v)	Tween 80 (% w/v)	Drug(mg)	Homogenization speed (rpm)	Homogenization time (min)	Stirring time (h)	Dispersion Volume (ml)
F1	50	150	50	0.50	-	-	20	1000	20	2	30
F2	50	125	75	0.50	-	-	20	1000	20	2	30
F3	50	50	150	0.50	-	-	20	1000	20	2	30
F4	50	75	125	0.50	-	-	20	1000	20	2	30
F5	50	100	100	0.50	-	-	20	1000	20	2	30
F6	50	100	100	-	-	0.50	20	1000	20	2	30
F7	50	100	100	-	0.50	-	20	1000	20	2	30
F8	50	100	100	0.50	-	-	20	1000	20	2	40
F9	50	100	100	0.50	-	-	20	1000	20	2	50
F10	50	100	100	0.50	-	-	10	1000	20	2	30
F11	50	100	100	0.50	-	-	30	1000	20	2	30
F12	50	100	100	0.10	-	-	20	1000	20	2	30
F13	50	100	100	0.30	-	-	20	1000	20	2	30
F14	50	100	100	1.00	-	-	20	1000	20	2	30
F15	50	100	100	0.50	-	-	20	700	20	2	30
F16	50	100	100	0.50	-	-	20	1300	20	2	30
F17	50	100	100	0.50	-	-	20	1000	10	2	30
F18	50	100	100	0.50	-	-	20	1000	30	2	30
F19	50	100	100	0.50	-	-	20	1000	20	2	30
F20	50	100	100	0.50	-	-	20	1000	20	0.5	30
F21	50	100	100	0.50	-	-	20	1000	20	1	30
F22	50	100	100	0.50	-	-	20	1000	20	3	30

2.1.2 Characterization of CA-LNs

Optimized CA-LNs in lyophilized form were characterized for particle size, polydispersity index (PDI), and zeta potential using photon correlation spectroscopy (Nano ZS, Malvern, UK). Test samples were dispersed in distilled water and further ultrasonicated for 30 seconds prior to testing.

Corresponding Author- Reetika Rawat, Shri Ram Murti Smarak, College of Engineering and Technology, Bareilly, 243202, India
reetikarawat32@gmail.com
Volume 17, Issue 1, 2026, Received: 15 Nov. 2025, Accepted: 5 Jan 2026, Published: 31 Jan 2026

Encapsulation efficiency was determined by determining the unencapsulated drug in the supernatant, obtained after centrifuging the CA-LNs dispersionat 25,000 rpm at 4°C for 20 minutes, using a UV/Visible spectrophotometer at 207 nm. Entrapment efficiency was calculated by using equation:

Entrapment efficiency (%) = (Total amount of drug –Free drug in supernatant) / Total amount of drug ×100

Further, surface morphology of the drug, physical mixture of the drug and formulation excipients, as well as the optimized CA-LNs, was examined using a field emission scanning electron microscope (MIRA3 TESCAN). Samples were placed to aluminum stubs with double-sided adhesive tape and sputter-coated with a gold-palladium alloy in an inert argon atmosphere prior capturing images at appropriate magnifications.

2.1.3 Dissolution studies

Optimized formulation was tested for *in-vitro* drug release in pH progressive media (HCl buffer pH 1.2 for 2 h followed by phosphate buffer pH 6.8) using modified dialysis bag diffusion method. Optimized CA-LNs equivalent to 10 mg of cefuroxime axitel were dispersed in 2.5 ml distilled water filled in dialysis bag (12 – 14 kDa) and immersed in dissolution medium (200 ml) maintained at 37 ± 2 °C and 100 rpm.Sink condition were maintained throughout the *in-vitro* release by adding 0.1% w/v sodium lauryl sulfate. Aliquots (3ml) were withdrawn at predetermined time intervalupto 24 h and each withdrawn volume was successively replaced with equal volume of fresh buffer. Further, aliquots were centrifuged and resultant supernatants were collected for analysis of cefuroxime axetil content using UV/Visible spectrophotometer at 281 nm.*In vitro* release data attained were plotted for various release kinetics models like zero order, first order, higuchi model and korsemeyer-peppas model to envisage the mechanism and kinetics of drug release. The best fit model was determined on the behalf of regression coefficient value.

2.1.4 Stability studies

For the determination of optimum storage conditions for CA-LNs, optimized lyophilized formulation was exposed to stability study according to guidelines of ICH for zone III and IV.Samples were stored in amber colored glass container screwed with caps under accelerated conditions (40 ± 2 °C/ 75 ± 5 % RH) for 6 months while for 12 months at room temperature (25 ± 2 °C/ 60 ± 5 % RH) and cool conditions (4 ± 2 °C/ 65 ± 5 % RH). Samples were withdrawn at an interval of 0, 1.5, 3, 6, 9 and 12 months for colloidal stability (particle size, PDI and zeta potential), entrapment efficiency and *in-vitro* release behavior of formulation. Lyophilized formulation was reconstituted with distilled water by vortexing before its evaluation. [22]

Corresponding Author- Reetika Rawat, Shri Ram Murti Smarak, College of Engineering and Technology, Bareilly, 243202, India
reetikarawat32@gmail.com
Volume 17, Issue 1, 2026, Received: 15 Nov. 2025, Accepted: 5 Jan 2026, Published: 31 Jan 2026

2.1.5 *In-vitro* anti-microbial study

The antimicrobial efficacy of the free drug and optimized CA-LNswas assessed against *E. coli* through antibacterial susceptibility testing and minimum inhibitory concentration (MIC) evaluation. Lyophilized bacterial test strains in the lag phase were cultivated in liquid nutrient broth and incubated at 37°C until the bacterial colony reached approximately 10^8 to 10^9 colony-forming units (CFU). The bacterial inoculum was diluted with sterile saline solution to meet the 0.5 McFarland standards.

Further, the antibacterial susceptibility test was performed utilizing the agar-well diffusion method (Sharma et al., 2016). Concisely, sterile nutrient agar plates were arranged and aseptically bored to prepare wells (5 mm in diameter). Cefuroxime axetil and CA-LNsconsisting drug equal to 50 µg/ml were aseptically applied in the repective wells, followed by the application of the corresponding bacterial culture (100 µl, 0.5 McFarland) utilizing a cotton swab. Further, the plates were then incubated for 24 hours at 37 °C. The sensitivity of the bacterial strain to cefuroxime axetil and CA-LNswas evaluated by measuring the zone of inhibition (ZOI). [22]

2.1.6 Determination of Minimum Inhibitory Concentration (MIC)

Growth inhibition of *E. coli* was estimated at the required minimum concentration, i.e. minimum inhibitory concentration (MIC) of cefuroxime axetil and CA-LNsequivalent to 0.7, 0.8, 0.9, 1, 2, 3, 4, 5, and 6 µg/ml were prepared. Concisely, sterile broth was inoculated with bacterial suspension (100 µl equivalent to the 0.5 McFarland standard), followed by the addition of various concentrations of the test samples. Further, all culture tubes were incubated at 37°C for 24 hours and analyzed for turbidity at 600 nm for detection of any bacterial growth. During the study Phosphate buffer saline was used as control. [22]

2.1.7 Determination of minimum biofilm inhibitory concentration (MBIC)

For determining the minimum biofilm inhibitory concentration, nutrient broth were inoculated with *E.Coli*, adjusted to 0.5 McFarland standards, and further incubated for 96 Hours at 37 °C to facilitate biofilm development. The broth was refreshed after 24 hrs, to eradicate non-adherent bacteria from the culture tubes. Moreover, biofilms that adhered to the walls and bottoms of the culture were rinsed with sterile distilled water two times for removal of any unattached bacteria. Following this, biofilm from the surfaces of the tubes was detached by adding 1 ml of sterile PBS, which was then subjected to sonication for 1 minute. The collected bacterial biofilms were treated with various concentrations of cefuroxime axetilor CA-LNs,corresponding to 30, 35, 40, 45, 50, 100, 130, 135, and 140 µg/ml of cefuroxime axetil, for 24 hours at 37 °C. Subsequently, the treated biofilms were incubated in fresh nutrient broth. The presence of viable organisms in

Corresponding Author- Reetika Rawat, Shri Ram Murti Smarak, College of Engineering and Technology, Bareilly, 243202, India
reetikarawat32@gmail.com
Volume 17, Issue 1, 2026, Received: 15 Nov. 2025, Accepted: 5 Jan 2026, Published: 31 Jan 2026

the culture tubes was assessed by measuring turbidity at 600 nm. [22] The biofilm assay was conducted in triplicate for each sample.

2.1.8 Statistical Analysis

The data is presented as mean ± SD (n=3). Statistical analysis was performed using one-way ANOVA followed by Bonferroni's multiple comparison test, utilizing GraphPad Prism version 5.00 (GraphPad Software, California, USA). A p-value of less than 0.05 was deemed statistically significant in all studies.

3. Results

Table 2: Effect of variables on PDI, Zeta potential, Zeta size and entrapment efficiency.

Corresponding Author- Reetika Rawat, Shri Ram Murti Smarak, College of Engineering and Technology, Bareilly, 243202, India
reetikarawat32@gmail.com
Volume 17, Issue 1, 2026, Received: 15 Nov. 2025, Accepted: 5 Jan 2026, Published: 31 Jan 2026

F.code	Particle size (nm)	PDI	Zeta Potential (mV)	Entrapment Efficiency (%)
F1	433.33± 37.27	0.412 ± 0.02	-16.7± 8.08	81.33± 1.83
F2	402.66± 23.86	0.35 ± 0.02	-25.4± 4.08	77± 1.75
F3	262.66± 39.46	0.18 ± 0.06	-17.7± 5.08	61± 2.26
F4	308± 37.89	0.25± 0.03	-26.32± 1.31	74.5± 0.68
F5	***335.11± 25.40***	***0.302± 0.06***	***-30.64± 3.58***	***86.02± 2.73***
F6	124.6± 17.78	0.754± 0.12	-14.6± 3.70	72.04± 3.74
F7	421.06± 41.2	0.875± 0.11	-27.11± 1.32	83.13± 1.06
F8	357.33± 34.07	0.327± 0.07	-19.6± 8.08	77.85± 3.38
F9	368.33± 37.98	0.387± 0.03	-18.3± 8.08	68.82± 2.41
F10	165.46± 25.01	0.305± 0.02	-14.76± 4.38	75.80± 6.94
F11	321.13± 38.83	0.413± 0.01	-21.63± 8.78	84.33± 1.17
F12	357.21± 8.08	0.547± 0.01	-18.91± 8.2	81.10±0.01
F13	345.33± 9.64	0.491± 0.01	-22.61± 8.6	81.97±0.02
F14	303.02± 7.04	0.316± 0.12	-21.81± 8.03	72.11± 2.21
F15	331.86± 10.53	0.292± 0.02	-20.03± 8.9	86.11±0.51
F16	473.66± 6.2	0.462± 0.03	-19.63± 8.2	75.33±1.89
F17	282.11± 4.8	0.182± 0.06	-17.7± 7.1	60.4± 1.78
F18	485.20± 6.1	0.413± 0.12	-20.82± 6.5	72.21± 3.21
F19	507.33±	0.557±	-17.94± 8.9	83.7±

Corresponding Author- Reetika Rawat, Shri Ram Murti Smarak, College of Engineering and Technology, Bareilly, 243202, India
reetikarawat32@gmail.com
Volume 17, Issue 1, 2026, Received: 15 Nov. 2025, Accepted: 5 Jan 2026, Published: 31 Jan 2026

	6.80	0.04		1.31
F20	452.60± 9.38	0.413± 0.01	-27.3± 8.4	84.73±2.45
F21	544.33± 5.03	0.254± 0.01	-20.4± 2.60	47± 0.84
F22	435.33± 37.27	0.402 ± 0.02	-16.7± 8.02	82.34± 1.81

3.1Formulation optimization

The significant variation in particle size and entrapment efficiency was noted with changes in lipid concentration. The average particle size and entrapment efficiency, when adjusting the stearic acid to glycerylbehenate ratio, ranged from 262.66 ± 39.46 nm to 433.33 ± 37.27 nm and from 61 ± 2.26 % to 81.30 ± 2.73% (refer to Table 2). An increase in glycerylbehenate content corresponded with enhanced entrapment efficiency and particle size (see Table 2). Nevertheless, a further increase in glycerylbehenate content beyond 50 % w/w of the total lipid did not yield any improvement in cefuroxime axetil loading, indicating a saturation effect of glycerylbehenate. An additional rise in glycerylbehenate content resulted in an increase in both particle size and PDI values, while entrapment efficiency decreased (as shown in Table 2).

Among the surfactants tested, pluronic F-68 produced smaller, uniformly dispersed particles (335.11 ± 25.40 nm) with a PDI of 0.302 ± 0.02 and a higher entrapment efficiency of 86.02 ± 2.73%. An increase in pluronic F-68 concentration from 0.1 % to 0.5 % w/v resulted in a reduction in particle size and an enhancement in entrapment efficiency (refer to Table 2). However, a further increase in pluronic F-68 concentration to 1% w/v led to the formation of a nanostructured carrier system characterized by smaller size and reduced entrapment efficiency (see Table 2). The polydispersity index (PDI) for all batches prepared with varying surfactant concentrations and types followed a similar trend to that of particle size.

When the drug to lipid ratio was varied from 1:25 to 1:12.5, an increase in encapsulation efficiency was observed. However, a further increase in the drug to lipid ratio to 1:8.33 resulted in a decrease in encapsulation efficiency due to a relatively smaller lipid proportion compared to the drug amount. This may have led to a higher diffusion of the drug into the continuous phase, thereby reducing encapsulation efficiency. An increase in the volume of the dispersion medium from 30 ml to 50 ml contributed to a decrease in entrapment efficiency, along with an increase in particle size and PDI (refer to Table 2).

Furthermore, increasing the homogenization speed from 12,500 rpm to 15,000 rpm resulted in an increase in particle size from 331.10 ± 25.40 nm to 473.66 ± 6 nm, while also decreasing the percentage of drug entrapment (refer to Table 2). Extending the homogenization time from 7.5 minutes to 20 minutes significantly reduced both particle size and polydispersity index (PDI), alongside enhancing encapsulation efficiency. However, a further increase to 30 minutes

Corresponding Author- Reetika Rawat, Shri Ram Murti Smarak, College of Engineering and Technology, Bareilly, 243202, India
reetikarawat32@gmail.com
Volume 17, Issue 1, 2026, Received: 15 Nov. 2025, Accepted: 5 Jan 2026, Published: 31 Jan 2026

introduced higher shear stress, which led to accelerated particle aggregation by rendering the system thermodynamically unstable (see Table 2).

Zeta potential, which quantitatively measures surface charge, plays a crucial role in determining the physical stability of the system. Batches prepared with various formulation and process parameters exhibited zeta potential values ranging from -14.7 ± 8.08 mV to -30.64 ± 3.58 mV. A zeta potential around ± 30 mV indicates a higher physical stability of the colloidal system.

Consequently, the formulation of CA-LNs(F5) was developed using optimized parameters, including a ratio of compritol to stearic acid of 1:1, pluronic F-68 at 0.5% w/v as a surfactant, a homogenization speed of 12,500 rpm, a homogenization duration of 20 minutes, and a continuous phase volume of 50 ml.

3.2 Solid state characterization

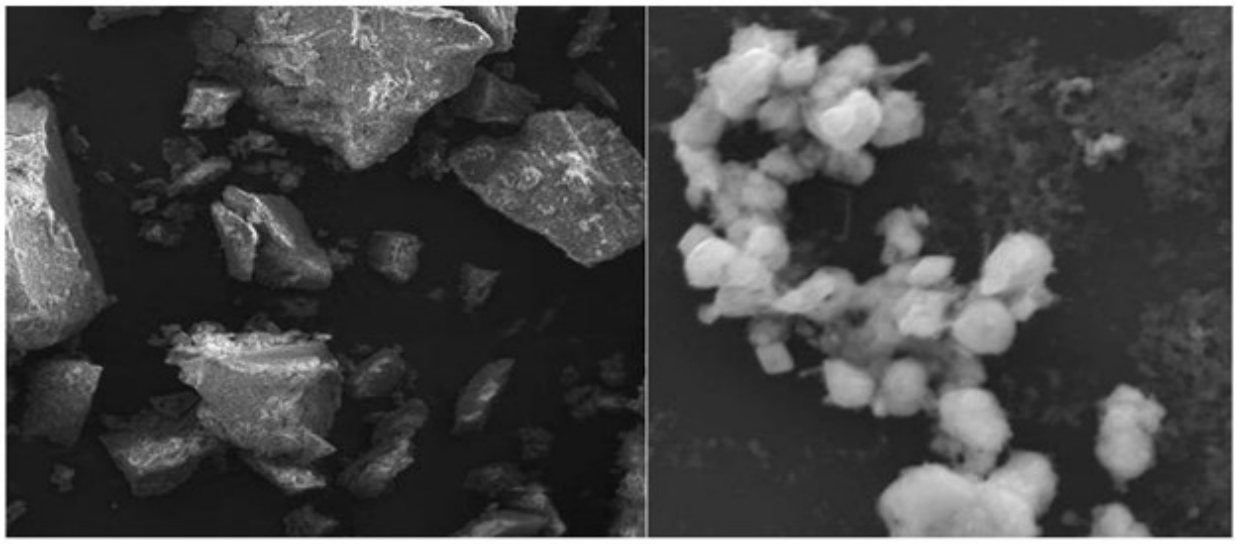

Figure1: Fe-SEM microphotographs of drug and formulation (CA-LCs)

A morphological analysis using Fe-SEM microphotographs revealed that cefuroxime axetil consists of oblong, cuboidal, cylindrical, and irregularly shaped particles with a varied size distribution. In contrast, CA-LNswere found to be homogeneous and spherical in shape, exhibiting a uniform size distribution. The surface of CA-LNsappeared smooth and free of cracks (Figure 1).

3.3 Dissolution study

Corresponding Author- Reetika Rawat, Shri Ram Murti Smarak, College of Engineering and Technology, Bareilly, 243202, India
reetikarawat32@gmail.com
Volume 17, Issue 1, 2026, Received: 15 Nov. 2025, Accepted: 5 Jan 2026, Published: 31 Jan 2026

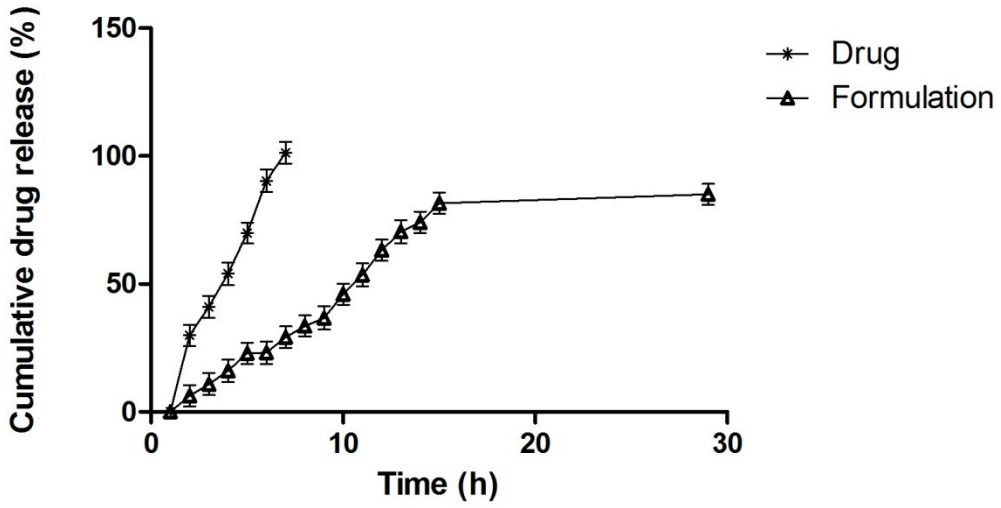

Figure 2:*In-vitro* release of drug (CA) and formulation (CA-LNs).

The cumulative percentage of cefuroxime axetil released *in-vitro* from the optimized CA-LNs (F5) under bio-relevant conditions of the gastrointestinal tract exhibited an initial burst release, specifically 24% drug release within 2 hours, followed by a gradual release over 24 hours (Figure 2). Additionally, the drug release mechanism and kinetics were assessed by applying the drug release data of CA-LNs to various release kinetic equations. The release data demonstrated the best fit with the Korseymeyer-Peppas equation, which was further validated by comparing the regression coefficients (R^2) of the zero-order (R^2 = 0.770), first-order (R^2 = 0.431), Higuchi model (R^2 = 0.928), and Korseymeyer-Peppas equation (R^2 = 0.988). The diffusion exponent value (n = 0.8642) confirmed the anomalous drug release pattern of CA-LNs**.**

3.4 Stability studies

Table 3: Stability study of optimized formulation at various temperatures.

S.No	Storage condition	Parameter	0M	1.5M	3M	6M	9M	12M
1	**Room temperature (25 ± 2 ° C/ 60 ± 5% RH)**	**Drug release (%) 24 h**	98.06 ±2.13	94.66 ±3.05	91.53 ±4.13	92.87 ±2.76	91.73 ±1.78	91.03 ±2.71
		E.E (%)	82.37 ±2.74	81.11 ±1.94	72.97 ±1.14	73.14 ±1.82	74.01 ±1.72	77 ±1.62

Corresponding Author- Reetika Rawat, Shri Ram Murti Smarak, College of Engineering and Technology, Bareilly, 243202, India
reetikarawat32@gmail.com
Volume 17, Issue 1, 2026, Received: 15 Nov. 2025, Accepted: 5 Jan 2026, Published: 31 Jan 2026

		Particle size (nm)	302.06 ±11.2	352.36 ±12.8	353.89 ±23.11	354.32 ±17.91	362.26 ±31.33	361.22 ±15.11
		PDI	0.195 ±0.08	0.194 ±0.03	0.205 ±0.08	0.221 ±0.16	0.224 ±0.02	0.238 ±0.08
		Zeta potential (mV)	-27.23 ±3.96	-27.61 ±2.36	-24.77 ±3.81	-24.78 ±2.73	-25.38 ±3.77	-25.13 ±2.71
2	**Cool Temperature (4 ± 2 °C/ 65 ± 5% RH)**	**Drug release (%) 24 h**	98.06 ±2.81	97.31 ±3.12	97.51 ±2.89	95.92 ±1.83	94.62 ±3.04	92.14 ±1.86
		E.E (%)	81.35 ±1.26	81.34 ±1.32	81.26 ±2.22	80.93 ±1.91	80.02 ±1.25	80.01 ±1.17
		Particle size (nm)	304.06 ±11.9	353.31 ±12.8	354.31 ±11.9	364.79 ±14.2	364.31 ±13.3	365.16 ±12.4
		PDI	0.191 ±0.02	0.192 ±0.01	0.194 ±0.04	0.202 ±0.02	0.214 ±0.03	0.225 ±0.04
		Zeta potential (mV)	-28.23 ±3.33	-28.78 ±2.91	-27.21 ±1.87	-25.07 ±2.61	-25.38 ±1.77	-24.67 ±1.81
3	**Accelerated Temperature (40 ± 2 °C/ 75 ± 5 % RH)**	**Drug release (%) 24 h**	98.06 ±2.12	97.76 ±3.02	95.08 ±2.19	91.84 ±2.16	-	-
		E.E (%)	81.39 ±1.28	77.12 ±1.33	77.14 ±1.04	74.04 ±1.86	-	-
		Particle size (nm)	304.06 ±11.21	362.12 ±13.4	365.32 ±10.8	374.91 ±16.7	-	-
		PDI	0.191 ±0.02	0.213 ±0.04	0.263 ±0.03	0.292 ±0.05	-	-
		Zeta potential (mV)	-28.23 ±3.18	-22.42 ±2.31	-21.34 ±2.91	-21.97 ±3.08	-	-

Table 3 presents the physicochemical characteristics of CA-LNs during the storage stability study. The physical appearance of CA-LNs did not exhibit any significant changes under various

Corresponding Author- Reetika Rawat, Shri Ram Murti Smarak, College of Engineering and Technology, Bareilly, 243202, India
reetikarawat32@gmail.com
Volume 17, Issue 1, 2026, Received: 15 Nov. 2025, Accepted: 5 Jan 2026, Published: 31 Jan 2026

environmental conditions. The optimized formulation (F5) stored under cool conditions (4 ± 2 °C/ 65 ± 5% RH) and at room temperature (25 ± 2 °C/ 60 ± 5% RH) showed no significant changes in particle size, PDI, zeta potential, entrapment efficiency, and in vitro release behavior after 12 months of storage ($p<0.05$). The stability results confirmed that the formulation and process variables were effectively optimized to produce stable CA-LNs. However, a significant increase in particle size and a decrease in entrapment efficiency, zeta potential, and drug release were observed under accelerated conditions after 6 months.

4. Discussion

The hot homogenization emulsification technique employed in the current study facilitated the direct incorporation of the physicochemically compromised lipophilic drug, cefuroxime axetil, while also eliminating the need for toxic organic solvents in the preparation of CA-LNs. [23, 24, 25, 26,27]

Preliminary investigations were conducted to optimize formulation parameters such as the ratio of stearic acid to glycerylbehenate, as well as the type and concentration of surfactant, with particle size, polydispersity index, and entrapment efficiency serving as benchmark criteria. Furthermore, the effects of manufacturing variables, including homogenization time, homogenization speed, and the volume of the external phase, were also examined.

Significant variations in particle size and entrapment efficiency were noted with changes in lipid concentration, attributed to differences in their HLB values. The presence of partial acylglycerols imparts amphiphilic properties to glycerylbehenate, aiding in the reduction of particle size. An increase in the proportion of glycerylbehenate within the lipid phase enhanced drug entrapment due to its complex nature and less ideal orientation, thereby providing additional space for drug loading. Moreover, the interchain interactions of behenic acid in glycerylbehenate and the incorporation of glycerylbehenate into the crystal lattice of stearic acid may have contributed to the fluidization of stearic acid chains, which could have improved the entrapment of cefuroxime axetil by creating more space within the NLCs. [28, 29.] Additionally, the relative increase in glycerylbehenate resulted in a rise in the viscosity of the organic phase, leading to a quicker solidification of nanoparticles, which in turn hindered the diffusion of cefuroxime axetil to the external phase. [30, 31] The diminished entrapment efficiency, along with the increase in particle size and polydispersity index (PDI) when the glycerylbehenate content exceeds 50% w/w, may be linked to a rise in interfacial tension between the lipid and aqueous phases, likely due to the heightened viscosity of the dispersed organic phase. Consequently, the coalescence of globules during the pre-emulsification phase led to an increase in particle size and the leaching of the encapsulated drug. [31-33]

Among the surfactants utilized in the study, the selection of surfactant for the preparation of CA-LNs was determined by their effects on particle size and entrapment efficiency. Pluronic F-68

Corresponding Author- Reetika Rawat, Shri Ram Murti Smarak, College of Engineering and Technology, Bareilly, 243202, India
reetikarawat32@gmail.com
Volume 17, Issue 1, 2026, Received: 15 Nov. 2025, Accepted: 5 Jan 2026, Published: 31 Jan 2026

may have aided in establishing a more compact mechanical and thermodynamic barrier at the interface of micelles, facilitating the formation of homogeneous nanosized particles with superior entrapment efficiency compared to Pluronic F-127 and Tween 80. The observation of smaller particle size and entrapment efficiency at elevated concentrations of Pluronic F-68 underscores the necessity of a significant amount of surfactant to create a stable colloidal system and to mitigate its solubilizing potential at higher concentrations. [34, 22, 33,35]

The insufficient shear magnitude experienced in a larger volume (50 ml) of continuous phase may be a factor contributing to the reduced entrapment efficiency and the increase in particle size and PDI. [22, 29, 36,37] The increase in shear force experienced by the system with the rise in homogenization speed may have expedited the coalescence or aggregation of the oil phase, resulting in larger particle size and PDI, alongside a decrease in entrapment efficiency and zeta potential. [38,39, 40] A homogenization time of 20 minutes facilitated the formation of uniform micellar structures. An extended duration of homogenization, however, generated greater shear force, which may have compromised the surfactant barrier and led to instability. [27, 7, 41] A higher zeta potential around ± 30 mV produces columbic forces of greater strength, which surpass the Van der Waals forces of attraction, thereby preventing aggregation. [21,18,42]

To assess the compatibility between cefuroxime axetil and the components of lipid nanoparticles (NLC), as well as to confirm the encapsulation of cefuroxime axetil in CA-LNs, initial evaluations were conducted using ATR-FTIR and DSC analyses. All peaks associated with cefuroxime axetil were detected in the ATR-FTIR spectrum of the physical mixture, indicating that cefuroxime axetil did not engage in any physicochemical interactions with the ingredients of CA-LNs. Additionally, the presence of distinct peaks for cefuroxime axetil in the ATR-FTIR spectrum, with only slight frequency changes compared to the pure drug, validated the successful encapsulation of cefuroxime axetilin LNs without any alterations during the fabrication process. Likewise, the characteristic endothermic peaks of all formulation components in the DSC thermogram of the physical mixture confirmed compatibility among the components. Conversely, the thermogram of CA-LNs, which lacked the melting endotherm of cefuroxime axetil, indicated a phase transition from crystalline to amorphous state during the encapsulation process, as well as a uniform dispersion of the drug within the formulation. [43-45] The morphological analysis further validated the smooth surface and spherical shape of CA-LNs.

The biphasic drug release profile, characterized by an initial burst release of approximately 24% of the drug within 2 hours, followed by a sustained release over 24 hours, was observed. The increased surface area provided by CA-LNsfor interaction with the dissolution fluid may have contributed to the enhanced diffusion and desorption of free or weakly bound cefuroxime axetil [46-48.] The gradual decline in the drug release rate could be attributed to the intrinsic solubility of

Corresponding Author- Reetika Rawat, Shri Ram Murti Smarak, College of Engineering and Technology, Bareilly, 243202, India
reetikarawat32@gmail.com
Volume 17, Issue 1, 2026, Received: 15 Nov. 2025, Accepted: 5 Jan 2026, Published: 31 Jan 2026

the drug, the distance the drug travels through the drug-depleted layers, the rigidity of the lipoidal barrier, and diffusion from the dialysis membrane. The extended release of the drug from the optimized formulation clearly indicates the improved efficacy and safety associated with the administration of cefuroxime axetil CA-LNs. Furthermore, kinetic modeling has validated the unusual drug release pattern of CA-LNs, which involves both dissolution and diffusion-controlled drug release through the lipid matrix.

The polymorphic transitions may have caused disturbances in the crystalline structure of lipids under accelerated storage conditions, leading to diminished stability. [27; 49; 50, 51, 52, 53, 54] Therefore, it is recommended that CA-LNs be stored at room temperature or in refrigerated conditions to preserve their pharmaceutical properties for effective long-term application.

4.1 *In vitro* anti-bacterial studies

The *in-vitro* antibacterial susceptibility test demonstrated that CA-LNs displayed superior antimicrobial activity against *E. coli*, a facultative anaerobic gram-negative bacterium. The determination of the minimum inhibitory concentration (MIC) indicated a greater effectiveness of the optimized formulation, showing a 6.7-fold increase against *E. coli* when compared to the free drug. [55, 56, 57, 58, 59, 60, 61, 62, 63, 64, 65] All concentrations utilized during the minimum biofilm inhibitory concentration (MBIC) assay exhibited an inhibitory effect on the growth of viable organisms. Likewise, the MBIC of the formulation was significantly lower, by 3.71-fold and 1.61-fold, than that of the pure drug against *E. coli* biofilms, respectively. This illustrates the enhanced effectiveness of cefuroxime axetil in the formulation within LNs. [66, 67, 68, 69, 70] The improved bactericidal activity of CA-LNs can be attributed to increased interactions, such as diffusion or fusion of CA-LNs with the bacterial cellular membrane, which facilitates direct drug delivery to the bacterial cytoplasm, along with the extended release of the drug from CA-LNs, functioning as a drug depot. [71,72]

4.1 *In vitro* anti-bacterial studies

The antimicrobial susceptibility test conducted on cefuroxime axetil demonstrated its superior antimicrobial effectiveness against *E. coli* (Zone of Inhibition: 9.2 mm). The optimized formulation (F5) exhibited a greater Zone of Inhibition when compared to the free drug against E. coli (14 mm), respectively.

The Minimum Inhibitory Concentration (MIC) values for cefuroxime axetil and the optimized formulation tested against *E. coli* were found to be 6 µg/ml and 0.9 µg/ml respectively. The lower MIC value of CA-LNsmay be attributed to their lipophilic nature and increased surface area facilitating interaction with microbial cells.

Corresponding Author- Reetika Rawat, Shri Ram Murti Smarak, College of Engineering and Technology, Bareilly, 243202, India
reetikarawat32@gmail.com
Volume 17, Issue 1, 2026, Received: 15 Nov. 2025, Accepted: 5 Jan 2026, Published: 31 Jan 2026

The formation of biofilm by *E. coli* was visually confirmed through the presence of a stained film on the walls of the test tube using the crystal violet staining method. Furthermore, SEM micrographs also validated the occurrence of biofilm formation (Figure 3). The enhanced anti-biofilm activity of CA-LNswas corroborated by SEM images, which indicated greater cell damage in comparison to the pure drug (Figure 3). The pure drug completely inhibited the growth of *E. coli* at concentrations of 130 µg/ml. In contrast, the optimized formulation achieved total eradication of bacterial growth from the biofilms of *E. coli* at concentrations of 35 µg/ml, respectively (Figure 3). Therefore, from a clinical perspective, CA-LNsrepresent a promising formulation as they may enhance the bioavailability of cefuroxime axetil, which is poorly soluble in water. [72]

Corresponding Author- Reetika Rawat, Shri Ram Murti Smarak, College of Engineering and Technology, Bareilly, 243202, India
reetikarawat32@gmail.com
Volume 17, Issue 1, 2026, Received: 15 Nov. 2025, Accepted: 5 Jan 2026, Published: 31 Jan 2026

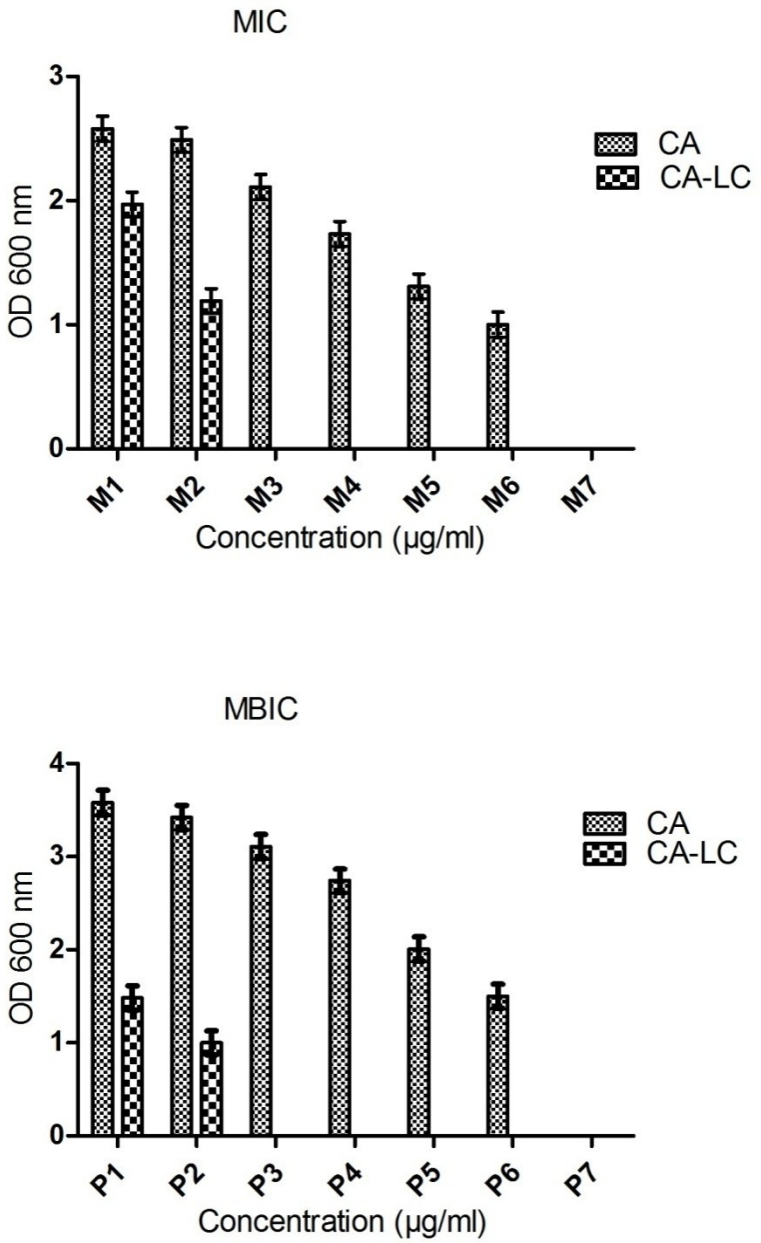

Figure 3: Minimum inhibitory concentration and minimum biofilm inhibitory concentration of drug (CA) cefuroxime axetil and optimized formulation (CA-LC) cefuroxime lipid nanocarriers against *E.coli*

5. Conclusion

Corresponding Author- Reetika Rawat, Shri Ram Murti Smarak, College of Engineering and Technology, Bareilly, 243202, India
reetikarawat32@gmail.com
Volume 17, Issue 1, 2026, Received: 15 Nov. 2025, Accepted: 5 Jan 2026, Published: 31 Jan 2026

In this study, the hot-homogenization method was employed to successfully incorporate cefuroxime axetil with a high entrapment efficiency. The fabricated CA-LNswere characterized physico-chemically and evaluated for their efficacy. The findings of this study demonstrate that CA-LNsare highly effective in eliminating biofilms formed by *E. coli* at lower concentrations than the drug itself. Stability studies indicated that CA-LNswould remain stable for up to one year of shelf life. Consequently, it can be concluded that cefuroxime axetil-loaded nanostructured lipid carriers can be regarded as a promising drug delivery system for biofilm eradication from cefuroxime axetil.

Declaration of competing interest: The authors declare that they have no known competing financial interests or personal relationships that could have appeared to influence the work reported in this paper.

References

1. Mack D, Becker P, Chatterjee I, et al. Mechanisms of biofilm formation in *Staphylococcus epidermidis* and *Staphylococcus aureus*: functional molecules, regulatory circuits, and adaptive responses. Int J Med Microbiol. 2004;294(2-3):203-212. doi:10.1016/j.ijmm.2004.06.015

2. Lewis K. Multidrug tolerance of biofilms and persister cells. Curr Top Microbiol Immunol. 2008;322:107-131. doi:10.1007/978-3-540-75418-3_6

3. Høiby N, Ciofu O, Bjarnsholt T. Pseudomonas aeruginosa biofilms in cystic fibrosis. Future Microbiol. 2010;5(11):1663-1674. doi:10.2217/fmb.10.125

4. Solleti VS, Alhariri M, Halwani M, Omri A. Antimicrobial properties of liposomal azithromycin for Pseudomonas infections in cystic fibrosis patients. J Antimicrob Chemother. 2015;70(3):784-796. doi:10.1093/jac/dku452

5. Contou D, Claudinon A, Pajot O, et al. Bacterial and viral co-infections in patients with severe SARS-CoV-2 pneumonia admitted to a French ICU. Ann Intensive Care. 2020;10(1):119. doi:10.1186/s13613-020-00736-x

6. Feldman C, Anderson R. The role of co-infections and secondary infections in patients with COVID-19. Pneumonia. 2021;13(1):5. doi:10.1186/s41479-021-00083-w

7. Lin C, et al. Nanoparticle-based drug delivery strategies in pharmaceutical sciences. J Pharm Sci. 2025;114(6):1569. doi:10.1016/j.xphs.2024.04.015

Corresponding Author- Reetika Rawat, Shri Ram Murti Smarak, College of Engineering and Technology, Bareilly, 243202, India
reetikarawat32@gmail.com
Volume 17, Issue 1, 2026, Received: 15 Nov. 2025, Accepted: 5 Jan 2026, Published: 31 Jan 2026

8. Pandit RS, Gaikwad SC, Agarkar GA, Gade AK, Rai M. Curcumin nanoparticles: physicochemical fabrication and in vitro efficacy against human pathogens. 3 Biotech. 2015;5(6):991-997. doi:10.1007/s13205-015-0302-9

9. Elkhatib W, Noreddin A. Efficacy of ciprofloxacin-clarithromycin combination against drug-resistant Pseudomonas aeruginosa biofilm. Microb Drug Resist. 2014;20(6):575-582. doi:10.1089/mdr.2014.0024

10. Sturaro M, et al. Advances in pharmacological approaches targeting microbial resistance. Front Pharmacol. 2024;15:11459926.

11. Iskandar I, Walters JD. Clarithromycin accumulation by phagocytes and its effect on killing of Aggregatibacter actinomycetemcomitans. J Periodontol. 2011;82(3):497-504. doi:10.1902/jop.2010.100221

12. Cepas V, López Y, Muñoz E, et al. Relationship between biofilm formation and antimicrobial resistance in Gram-negative bacteria. Microb Drug Resist. 2019;25(1):72-79. doi:10.1089/mdr.2018.0027

13. Üsküdar O, et al. Clinical outcomes in hepatology patients receiving antimicrobial therapy. Ann Hepatol. 2010;9(4):—

14. Ramalingam P, Ko YT. Enhanced oral delivery of curcumin from surface-modified solid lipid nanoparticles: pharmacokinetic and brain distribution studies. Pharm Res. 2015;32(2):389-402. doi:10.1007/s11095-014-1469

15. Chinthaginjala H, et al. Pharmaceutical nanoparticle systems for improved bioavailability. Indian J Pharm Educ Res. 2024;58(1):21-33. doi:10.5530/ijper.58.1.3

16. Baek JS, Cho CW. Surface modification of solid lipid nanoparticles enhances oral curcumin bioavailability. Eur J Pharm Biopharm. 2017;117:232-240. doi:10.1016/j.ejpb.2017.04.013

17. Khan I, et al. Emerging nanotherapeutics in antimicrobial drug delivery. Front Pharmacol. 2022;13:10460807.

18. Naeiji A, et al. Advanced interfaces for biomedical nanoparticle applications. Adv Mater Interfaces. 2024;11(14):2400496. doi:10.1002/admi.202400496

Corresponding Author- Reetika Rawat, Shri Ram Murti Smarak, College of Engineering and Technology, Bareilly, 243202, India
reetikarawat32@gmail.com
Volume 17, Issue 1, 2026, Received: 15 Nov. 2025, Accepted: 5 Jan 2026, Published: 31 Jan 2026

19. dos Santos Ramos MA, da Silva PB, Spósito L, et al. Nanotechnology-based drug delivery systems for microbial biofilm control. Int J Nanomedicine. 2018;13:1179-1213. doi:10.2147/IJN.S146195

20. Panthi K, et al. Novel pharmaceutical nanocarriers for controlled drug release. Eur J Pharm Sci. 2024;192:106498. doi:10.1016/j.ejps.2024.106498

21. Sharma M, Sharma V, Panda AK, Majumdar DK. Development and evaluation of pharmaceutical lipid nanoparticles. Pharm Dev Technol. 2013;18(3):560-569. doi:10.3109/10837450.2011.604782

22. Sharma M, Gupta N, Gupta S. Designing clarithromycin-loaded solid lipid nanoparticles: pharmacokinetics, antibacterial activity, and safety. RSC Adv. 2016;6(80):76621-76631. doi:10.1039/C6RA12841F

23. Mehnert W, Mäder K. Solid lipid nanoparticles: production, characterization and applications. Adv Drug Deliv Rev. 2020;47:165-196.

24. Xie S, Zhu L, Dong Z, Wang X, Wang Y, Li X, Zhou W. Preparation and characterization of lipid-based nanoparticles. Colloids Surf B Biointerfaces. 2011;83(2):382-387. doi:10.1016/j.colsurfb.2010.12.014

25. Sharma M, Chaudhary D. Advances in nanomedicine-based drug delivery systems. Nanomedicine. 2022;42:102543. doi:10.1016/j.nano.2022.102543

26. Kumar A, et al. Nanotechnology approaches for enhanced antimicrobial therapy. ACS Omega. 2023;8(28):25239. doi:10.1021/acsomega.3c02239

27. Sharma M, Sharma S, Wadhwa J. Artificial cells and nanobiotechnology in drug delivery. Artif Cells Nanomed Biotechnol. 2019;47(1):45-55. doi:10.1080/21691401.2018.1543191

28. Aburahma MH, Badr-Eldin SM. Lipid nanoparticles in oral drug delivery. Expert Opin Drug Deliv. 2014;11(12):1865-1883. doi:10.1517/17425247.2014.935335

29. Zhang Y, et al. Advanced lipid carriers for pharmaceutical applications. Eur J Pharm Sci. 2025;195:106789. doi:10.1016/j.ejps.2025.106789

30. Khalil RM, El-Bary AA, Kassem MA, Ghorab MM, Basha M. Formulation of nanoparticle drug systems. Egypt Pharm J. 2013;12:63-72. doi:10.7123/01.EPJ.0000428643.74323.d9

Corresponding Author- Reetika Rawat, Shri Ram Murti Smarak, College of Engineering and Technology, Bareilly, 243202, India
reetikarawat32@gmail.com
Volume 17, Issue 1, 2026, Received: 15 Nov. 2025, Accepted: 5 Jan 2026, Published: 31 Jan 2026

31. Chokshi NV, Khatri HN, Patel MM. Controlled-release lipid nanoparticle formulations. Drug Dev Ind Pharm. 2018;44(12):1975-1989. doi:10.1080/03639045.2018.1506472

32. Duong TH, et al. Nanomedicine strategies for drug delivery optimization. Int J Nanomedicine. 2020;15:7587-7569.

33. Rarokar NR, et al. Lipid nanocarriers for antimicrobial applications. J Mol Liq. 2024;392:1223819. doi:10.1016/j.molliq.2022.1223819

34. Ojha S, Kumar B. Pharmaceutical nanotechnology advances in therapy. Adv Pharm Bull. 2018;8(2):225-233. doi:10.15171/apb.2018.027

35. Mm T, Abdul M, Othman M. Hepatoprotective effects of clove extract in rats. J HerbMedPharmacol. 2018;7:1-10.

36. Singh B, Vuddanda PR, Rao M, Kumar V, Saxena PS, Singh S. Cefuroxime-loaded solid lipid nanoparticles against Staphylococcus aureus biofilm. Colloids Surf B Biointerfaces. 2014;121:92-98. doi:10.1016/j.colsurfb.2014.03.046

37. Singh AK, Mukerjee A, Pandey H, Mishra SB. Fabrication and optimization of solid lipid nanoparticles by Box–Behnken design. J Appl Pharm Sci. 2021;11(9):35-47. doi:10.7324/JAPS.2021.110905

38. Adelli GR, Balguri SP, Bhagav P, Raman V, Majumdar S. Sustained-release ocular films for drug delivery. Drug Deliv. 2017;24(1):370-379. doi:10.1080/10717544.2016.1256000

39. Abdelhamed H, Ibrahim I, Baumgartner W, Lawrence ML, Karsi A. Histopathological changes in catfish infected with Aeromonas hydrophila. Front Microbiol. 2017;8:1519. doi:10.3389/fmicb.2017.01519

40. Hassanen EI, Khalaf AA, Tohamy AF, Mohammed ER, Farroh KY. Toxicopathological studies of chitosan-coated silver nanoparticles in rats. Int J Nanomedicine. 2019;14:4723-4739. doi:10.2147/IJN.S207644

41. Araghi A, Golshahi H, Baghban F, Tabari MA. Farnesol against cyclophosphamide toxicity in mice. J HerbMedPharmacol. 2018;7(1):37-43. doi:10.15171/jhp.2018.07

42. Hermida MER, de Melo CVB, Lima IS, et al. Histological disorganization in visceral leishmaniasis. Front Cell Infect Microbiol. 2018;8:394. doi:10.3389/fcimb.2018.00394

Corresponding Author- Reetika Rawat, Shri Ram Murti Smarak, College of Engineering and Technology, Bareilly, 243202, India
reetikarawat32@gmail.com
Volume 17, Issue 1, 2026, Received: 15 Nov. 2025, Accepted: 5 Jan 2026, Published: 31 Jan 2026

43. Singhal A, Aliouat EM, Hervé M, et al. Experimental tuberculosis model in Wistar rats. PLoS One. 2011;6(4):e18632. doi:10.1371/journal.pone.0018632

44. Nagaraj S, Arulmurugan P, Karuppasamy K, et al. Hepatoprotective effects of C-phycocyanin in rats. Acad J Cancer Res. 2011;4(2):29-34.

45. Labro MT, Benna JE, Babin-Chevayec C. Effects of macrolides on oxidative burst in neutrophils. J Antimicrob Chemother. 1989;24(4):561-572. doi:10.1093/jac/24.4.561

46. Giamarellos-Bourboulis EJ, Antonopoulou A, Raftogiannis M, et al. Immunomodulatory effects of clarithromycin in pyelonephritis. BMC Infect Dis. 2006;6:31. doi:10.1186/1471-2334-6-31

47. Giamarellos-Bourboulis EJ, Adamis T, Laoutaris G, et al. Clarithromycin treatment of experimental sepsis. Antimicrob Agents Chemother. 2004;48(1):93-99.

48. Hardy RD, Rios AM, Chavez-Bueno S, et al. Clarithromycin in Mycoplasma pneumoniae pneumonia model. Antimicrob Agents Chemother. 2003;47(5):1614-1620.

49. Ghaffari S, Varshosaz J, Saadat A, Atyabi F. Amikacin-loaded solid lipid nanoparticles. Int J Nanomedicine. 2011;6:35-43. doi:10.2147/IJN.S13671

50. Cholakova D, Denkov ND. Advances in colloid and interface science. Adv Colloid Interface Sci. 2024;318:102938. doi:10.1016/j.cis.2023.102938

51. Beasley MB. Acute lung injury—from cannabis to COVID. Mod Pathol. 2022;35:1-7. doi:10.1038/s41379-021-00915-6

52. Singh R, et al. Nanotechnology-based pharmaceutical systems. Front Pharmacol. 2021;12:8460681.

53. Qi L, Li H, Zhang C, et al. Antibiotic resistance and biofilm formation in Acinetobacter baumannii. Front Microbiol. 2016;7:483. doi:10.3389/fmicb.2016.00483

54. Inoue Y, Yoshimura S, Tozuka Y, et al. Solubilization of clarithromycin using ascorbic acid glucoside. Int J Pharm. 2007;331(1):38-45. doi:10.1016/j.ijpharm.2006.09.014

55. Sharma M, Chaudhary D. Lipid nanoparticles for enhanced drug delivery. Int J Pharm. 2021;594:120176. doi:10.1016/j.ijpharm.2020.120176

Corresponding Author- Reetika Rawat, Shri Ram Murti Smarak, College of Engineering and Technology, Bareilly, 243202, India
reetikarawat32@gmail.com
Volume 17, Issue 1, 2026, Received: 15 Nov. 2025, Accepted: 5 Jan 2026, Published: 31 Jan 2026

56. Sahay G, Alakhova DY, Kabanov AV. Polymeric micelles in drug delivery. J Control Release. 2010;145(3):182-195. doi:10.1016/j.jconrel.2010.01.036

57. Cai S, Yang Q, Bagby TR, Forrest ML. Nanoparticles in therapeutic delivery. Adv Drug Deliv Rev. 2011;63(10-11):901-908. doi:10.1016/j.addr.2011.05.017

58. Dash S, Murthy PN, Nath L, Chowdhury P. Pharmaceutical dissolution techniques. Acta Pol Pharm. 2010;67(3):217-223.

59. Grassi M, Voinovich D, Franceschinis E, et al. Controlled release pharmaceutical systems. J Control Release. 2003;92(3):275-289. doi:10.1016/S0168-3659(03)00330-4

60. Tatke A, Dudhipala N, Janga KY, et al. Nanomaterials in ocular drug delivery. Nanomaterials. 2019;9(1):3. doi:10.3390/nano9010003

61. Li N, Li X, Cheng P, et al. Herbal therapeutics in disease management. Evid Based Complement Alternat Med. 2021;2021:4828169. doi:10.1155/2021/4828169

62. Ranjan S, Dasgupta N, Verma P, Ramalingam C. Nanomaterial applications in chemistry. J Indian Chem Soc. 2020;97:483-491.

63. Bulcão RP, Freitas FA, Venturini CG, et al. Toxicological effects of nanoparticles. Toxicol Sci. 2013;132(1):162-176. doi:10.1093/toxsci/kfs334

64. Yang J, Li W, Duan M, et al. Ketamine inhibits acute lung injury in rats. Inflamm Res. 2005;54(3):133-137. doi:10.1007/s00011-004-1334-5

65. Halim RMA, Kassem NN, Mahmoud BS. Biofilm-producing staphylococci and methicillin resistance. Open Access Maced J Med Sci. 2018;6(8):1335-1341. doi:10.3889/oamjms.2018.246

66. Shao L, Takeda K, Kato S, Mori S, Kodama T. Lymphatic and venous system communication in mice. J Immunol Methods. 2015;424:100-105. doi:10.1016/j.jim.2015.05.007

67. Moghimi SM, Hunter AC, Andresen TL. Nanoparticle pharmacokinetics. Annu Rev Pharmacol Toxicol. 2012;52:481-503. doi:10.1146/annurev-pharmtox-010611-134623

68. Solleti VS, Alhariri M, Halwani M, Omri A. Liposomal azithromycin antimicrobial activity. J Antimicrob Chemother. 2015;70(3):784-796. doi:10.1093/jac/dku452

Corresponding Author- Reetika Rawat, Shri Ram Murti Smarak, College of Engineering and Technology, Bareilly, 243202, India
reetikarawat32@gmail.com
Volume 17, Issue 1, 2026, Received: 15 Nov. 2025, Accepted: 5 Jan 2026, Published: 31 Jan 2026

69. Bikiaris ND, Ainali NM, Christodoulou E, et al. Hybrid nanocarriers for paclitaxel delivery. Nanomaterials. 2020;10(12):2490. doi:10.3390/nano10122490

70. Xi Z, Zhang W, Fei Y, et al. Pharmaceutical nanocarrier systems. Pharmaceutics. 2020;12(2):144. doi:10.3390/pharmaceutics12020144

71. Jeengar MK, Rompicharla SVK, Shrivastava S, et al. Emu oil nano-emulgel for curcumin delivery. Int J Pharm. 2016;506(1-2):222-236. doi:10.1016/j.ijpharm.2016.04.05

72. Shukla P, Dwivedi P, Gupta PK, Mishra PR. Tocopheryl acetate nanoemulsions for curcumin in sepsis therapy. Expert Opin Drug Deliv. 2014;11(11):1697-1712. doi:10.1517/17425247.2014.932769

Corresponding Author- Reetika Rawat, Shri Ram Murti Smarak, College of Engineering and Technology, Bareilly, 243202, India
reetikarawat32@gmail.com
Volume 17, Issue 1, 2026, Received: 15 Nov. 2025, Accepted: 5 Jan 2026, Published: 31 Jan 2026